Development and Simulation of 26 GHz Beamforming Systems and Antenna Array 5G Network Base Stations

Abd Al Menam A. Alazzawi, Mohamad Kamal A. Rahim, and Osman Ayop

Advanced RF & Microwave Research Group (ARFMRG)
Faculty of Electrical Engineering, University Technology Malaysia (UTM), 81310 UTMJB Johor, Malaysia
abdalmenamahmed6@gmail.com, mdkamal@utm.my, osmanayop@utm.my

Abstract – This paper focuses on designing a new structure of beamforming networks with an array antenna to control the beams. The 3×4 array antenna structure connects to the 3×3 Rotman lens beamformers to achieve this goal. The middle time delay line is around 14 mm. The design allows the *x*-axis to cover +25, 0, −25 degrees. Therefore, this work targets fifth generation (5G) application, which necessitates coverage in all directions by other base stations or users. Computer Simulation Technology (CST) microwave software facilitates the simulation process. The design begins with a single microstrip patch antenna, designed to function as an array antenna resonating at 26 GHz. The half-lambda separation (λ/2) among antennas gives 13.8 dBi gain with S11< −10 dB. The final structure for beamforming networks has a gain of 14 dBi. This work uses the Roger 5880 substrate, which has a dielectric constant of 2.2, a loss tangent of 0.0009, and a thickness of 0.127 mm.

Index Terms – array antenna, CST studio, mm-wave, Rotman lens, series feed antenna.

I. INTRODUCTION

The introduction of fifth generation (5G) wireless communication technology marks a significant advancement in mobile wireless communication systems [1]. Positioned as a notable improvement over previous generations, 5G aims to enhance data transmission rates, reduce latency, and increase the capacity for interconnected devices. Engineered to support various applications such as virtual reality, autonomous vehicles, smart cities, and the Internet of Things (IoT), 5G technology integrates high-frequency radio waves, advanced antenna technologies, and network virtualization [2, 3]. An important challenge faced by array antennas equipped with beamforming circuits relates to coverage direction, particularly in addressing blind angles and optimizing beamforming for wider radiation. In response, series-feed array antennas offer a flexible solution by allowing the adjustment of beam patterns through modulation of signal phase and amplitude, often with the assistance of a beamformer. Furthermore, integrating a Rotman lens (an effective microwave lens capable of directing electromagnetic waves) can improve the performance of series-fed array antennas [4]. The effectiveness of Rotman lens design relies on careful consideration of factors such as frequency range, lens geometry, material composition, and relevant parameters. When combined with a series-fed array antenna, the Rotman lens is typically positioned at the array's focal point to concentrate electromagnetic waves emitted by array elements, thereby enhancing antenna system gain and directivity [5]. Series-fed array antennas with Rotman lenses find applications in various fields, including 5G wireless communication, radar systems, and remote sensing, especially in scenarios requiring precise energy transmission or reception [6, 7].

This paper delves into the design of series-fed array antennas integrated with Rotman lenses, specifically resonating at 26 GHz, for application in fifth-generation wireless communication networks. The primary objective is to address unseen and blind angles within the coverage area. Computer Simulation Technology (CST) software is employed for simulation and prototype design purposes. The substrate material selected for this simulation is Rogers 5880, featuring a thickness of 0.127 mm.

II. PROPOSED ROTMAN LENS DESIGN

Rotman lenses play a pivotal role in microwave engineering, facilitating precise manipulation of electromagnetic waves through focusing and beam steering mechanisms [8]. Researchers extensively utilize a sophisticated set of equations to ascertain crucial aspects of the lens, including its geometry, dimensions, material composition, and thickness [9, 10]. These calculations are indispensable for attaining the desired performance parameters necessary for optimal functionality and efficiency in various applications [11, 12]. Figure 1 illustrates how the link technique demonstrates the connections between different components in the system, offering insightful information on the internal mechanisms of Rotman lens-integrated setups [13, 14].

The design process of the printed Rotman lens began by establishing the dimensions of the transmission line,

Submitted On: May 2, 2024
Accepted On: June 13, 2024

https://doi.org/10.13052/2024.ACES.J.390505

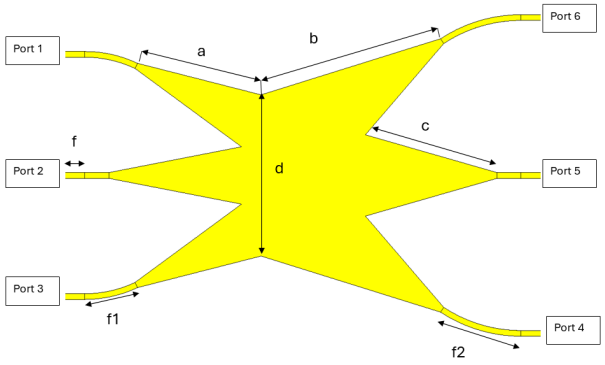

(a)

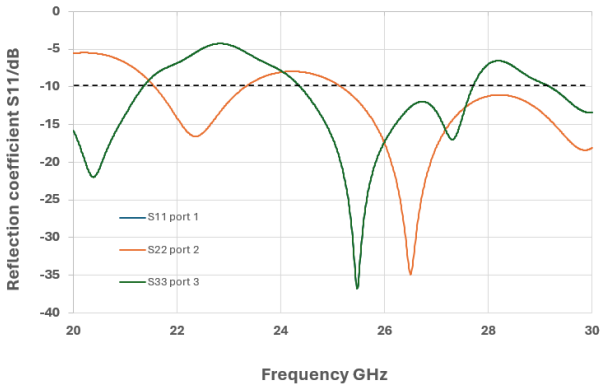

(b)

Fig. 1. (a) Structure of a 3×3 Rotman lens and (b) reflection coefficient for the Rotman lens's input ports.

denoted as Wr (transmission line width) and Lr (transmission line length):

$$Wr = \frac{(c*2*f)}{\sqrt{\varepsilon r} - (\sin 2\theta)}, \tag{1}$$

$$Lr = \frac{(c*2*f)}{(2*\sqrt{\varepsilon r} - \sin 2\theta)}, \tag{2}$$

$$d = L*\sqrt{n}-1). \tag{3}$$

Equation (3) determines the position of the feed network by calculating the distance between it and the first transmission line. This calculation involves considering the width (Wr) and length (Lr) of the transmission line, the speed of light (c), the operating frequency (f), the relative permittivity of the substrate (εr), and the beam scanning angle (θ):

$$S = Wr*\tan\left(\frac{\theta}{2}\right). \tag{4}$$

The position of the radiating elements is determined using equation (4), where S represents the element spacing, Wr is the width of the transmission line, and θ denotes the beam scanning angle. This equation plays a crucial role in establishing the precise placement of the radiating elements in the system, ensuring optimal performance and functionality:

$$x = (n-1)*S*\sin(\theta). \tag{5}$$

The position of the i-th radiating element, denoted by x, in an array of n transmission lines with an element spacing of S is crucial in determining the beam scanning angle, represented by θ as shown in equation (5). The relationship between these parameters is fundamental to the design and analysis of antenna arrays for various applications in wireless communication and radar systems [15, 16]. The precise calculation and adjustment of these values in Table 1 are essential to achieving the antenna array's desired radiation pattern and beam steering capabilities.

Table 1: Dimension of Rotman lens design structure (all dimensions are in mm)

Dimensions	Value (mm)
a	8.67
b	12.78
c	9.30
d	10.94
f	1.63
f1	3.66
f2	5.70

III. SERIES FEED ARRAY ANTENNA DESIGN AT 26 GHz

A. Microstrip patch antenna

A pre-established formula is implemented during the fabrication process of microstrip antennas. Equations (6–10) provide a representation of the antenna's equation:

$$wp = \frac{c}{2fo\sqrt[2]{\frac{(\varepsilon r+1)}{2}}}, \tag{6}$$

$$Leff = \frac{c}{2fo\sqrt[2]{\varepsilon reff}}, \tag{7}$$

$$\varepsilon reff = \frac{\varepsilon r+1}{2} + \frac{\varepsilon r-1}{2}\left[1+12\frac{h}{wp}\right]^{-\frac{1}{2}}, \tag{8}$$

$$\Delta L = 0.412h\frac{(\varepsilon reff+0.3)\left(\frac{wp}{h}+0.264\right)}{(\varepsilon reff-0.258)\left(\frac{wp}{h}+0.8\right)}, \tag{9}$$

$$Lp = Leff - 2\Delta L. \tag{10}$$

Initially, equation (6) is employed to determine the width of the patch, denoted as Wp, predicated on key parameters such as the resonant frequency (fr), relative permittivity (εr), and substrate height (h). Subsequently, equation (8) is utilized to derive the effective permittivity, ε_{reff}, crucial for computing the length extension, ΔLp, attributed to fringing fields, contingent upon the condition $Wp/h>1$ as delineated in equation (9). Finally,

equation (10) facilitates the calculation of the patch length, *Lp*, completing the design process with meticulous precision.

B. Series feed array antenna

To successfully integrate a Rotman lens with a series-fed array antenna operating at 26 GHz, it is crucial to meticulously assess the antenna's frequency range and bandwidth, along with the configuration of the array consisting of four elements spaced at half a wavelength. The choice of elements in the array significantly influences the antenna's performance metrics such as gain, directivity, and bandwidth [17, 18].

Figure 2 and Table 2 provides insight into the (W_p *x* L_p) series feed structure and its corresponding equivalent circuit with 3.89 mm separation distance which is λ/2. It's printed over Roger 5880 substrate with 2.2 dielectric constant and 0.127 mm substrate thickness to radiate at 26 GHz.

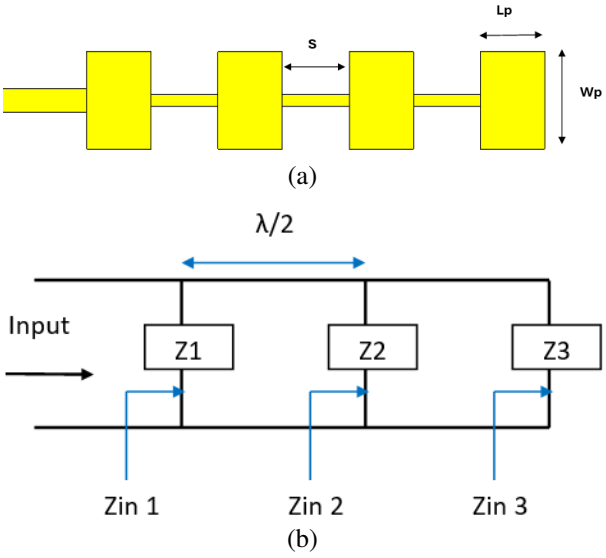

Fig. 2. Microstrip series feed patch antenna (a) 1×4 series feed antenna and (b) equivalent circuit of series feed antenna.

Employing a series feed array configuration yielded a substantial gain enhancement, elevating the gain from approximately 8.5 dBi to approximately 14 dBi.

Table 2: Microstrip series feed array antennas dimensions (all dimensions in mm)

Dimensions	Value (mm)	Explanation
Wp	4.80	Patch Width
Lp	3.65	Patch Length
S	3.89	Elements Spacing
h	0.127	Substrate Hight
εr	2.2	Epsilon

Additionally, fine-tuning of the bandwidth allocation facilitated the generation of a single beam transmitting at 26 GHz, thereby enhancing signal efficiency. These advancements are visually elucidated in the accompanying schematic in Fig. 3 (a,b).

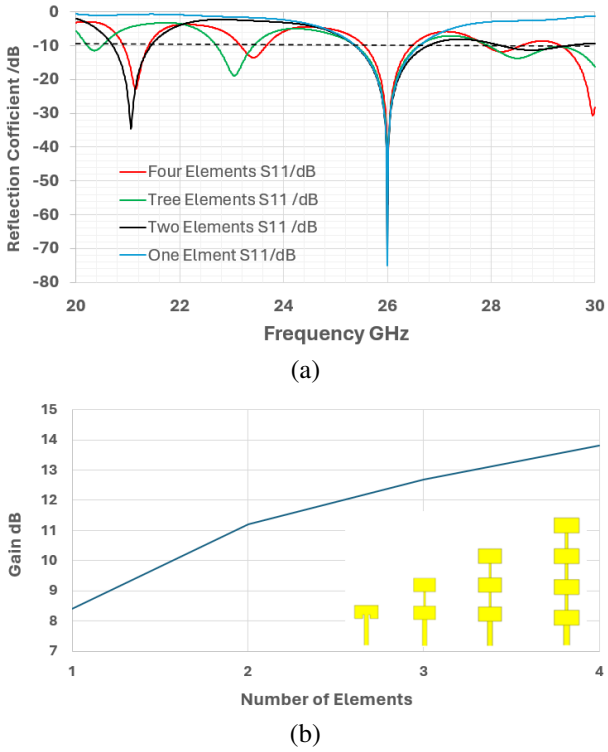

Fig. 3. (a) Reflection coefficient for single patch to four series feed antennas and (b) gain of single patch to four elements series feed antennas.

IV. RESULTS AND DISCUSSIONS

In the design process, the series feed antennas are fabricated using Roger 5880 material to ensure resonance at 26 GHz. In order to verify the accuracy of the antenna fabrication, the reflection coefficient and radiation pattern were measured, as shown in Fig. 4 (a, b).

The proposed structure is simulated using CST software, and the performance is monitored by the reflection coefficient (S11), gain, bandwidth, and radiation pattern. Figure 5 shows the integration of an array antenna with a Rotman lens over 80 by 31 mm using a 13-14 mm delay line to achieve a phase difference based on the True Time Delay (TDD) concept of the Rotman lens [19, 20]. Figure 6 shows the reflection coefficient S11 of the integrated final structure. From the analysis, the reflection coefficient is less than 15 dB. Synchronization between the array antennas and the beamforming network is achieved by a 3×3 Rotman lens set by resonating at the same frequency. The connected Rotman lens was

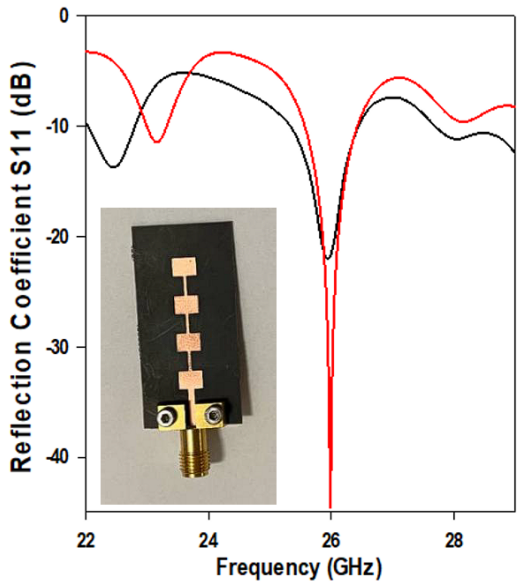

(a)

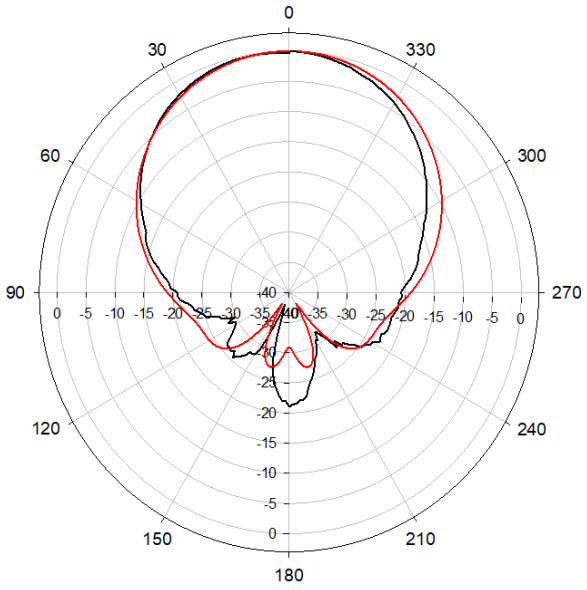

(b)

Fig. 4. (a) Fabricated series feed array antennas with reflection coefficient and (b) radiation pattern comparison (phi=0).

prepared to shift the phase at −25, 0, +25 degrees. The array antennas have connected single-layer 0.127 mm Rotman beamformers to allow the beam to cover blinded angles efficiently [21, 22].

The radiation pattern of the proposed final structure depicted in Fig. 7 is analyzed at 26 GHz with Phi=0 deg. The beam is observed to have a beam at −25, 0, and +25 degrees, with the gain of ports 1 to 3 around 14.2 dBi. The beams exhibit an angular width (3 dB) ranging from 20 to 30 degrees.

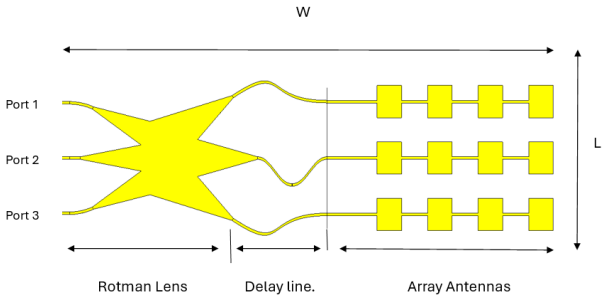

Fig. 5. Integrated structure of 3×3 Rotman lens and 3×4 array antennas.

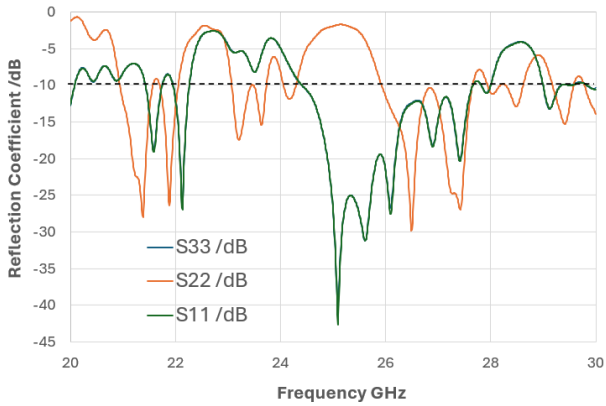

Fig. 6. Reflection coefficient S11 of integrated final structure of Rotman lens and array antennas.

The results presented in Table 3 exhibit a strong alignment with prominent references in the field, showcasing the efficiency of this particular structure in identifying broad blinded angles that were previously unaddressed by alternative designs. Notably, the comparison highlights the remarkable capability of this configuration to attain 0 and ±25 degrees utilizing merely three input ports. This significant breakthrough accentuates

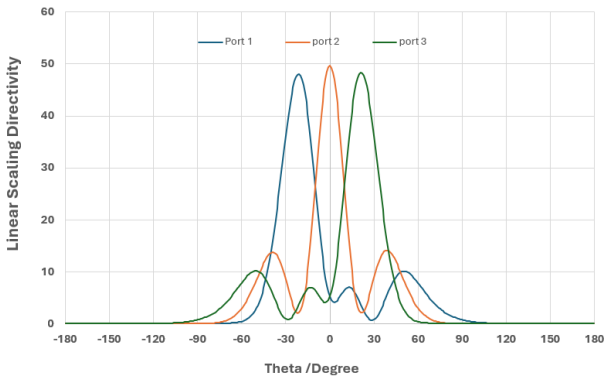

(a)

Fig. 7. (*Continued.*)

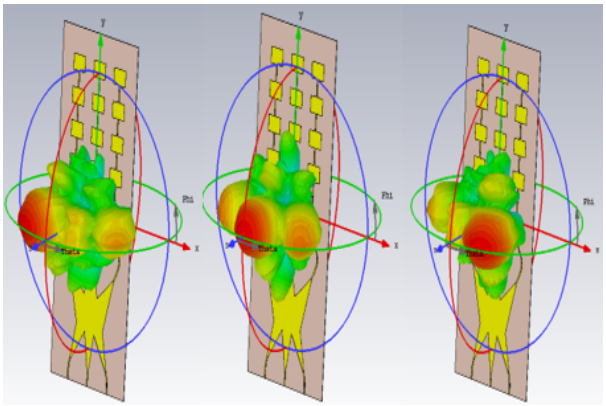

(b)

Fig. 7. Radiation pattern of final structure (a) directivity using Cartesian coordinate and (b) 3D radiation pattern.

the considerable potential for further advancements and the implementation of optimizations tailored to specific applications.

Table 3: Performance of final structure in comparison with other references

Variables	This Work	Ref (11)	Ref (13)	Ref (16)
Frequency GHz	26	6-18	60	10-14
Return Loss dB	20	16	12	25
Gain dB (Max)	14.2	-	-	11.37
Beam angle (deg)	0±25	0±28	0±25	0±16
Subs thickness (mm)	0.127	-	0.127	0.0027
No. of input ports	3	8	5	11

V. CONCLUSION

The microstrip series feed patch antenna is operated at 26 GHz with a separation of half lambda. A single-series-fed patch antenna is enhanced into a 3×4 array antenna configuration. To widen the coverage angle and improve sensitivity, 3×3 Rotman lenses were designed. A beamforming network circuit was meticulously devised to match the array of antenna ports, incorporating a delay line with 14 mm separations. This novel structure aims to eliminate blind angles effectively. The array antennas demonstrated a gain of 14 dBi and a reflection coefficient of 20 dB or less, showcasing their high performance. The precise beam control of the array, coupled with the Rotman lenses, enables coverage of angles from −25 to +25 degrees along the *x*-axis. This advancement makes the antennas suitable for applications in 5G and automotive radar systems. For future improvements, integrating a programmable controller chip could further optimize beam characteristics based on specific application requirements.

ACKNOWLEDGMENT

The authors thank, Research Management Center (RMC), Universiti Teknologi Malaysia (UTM), Faculty of Electrical Engineering for the support of the research under grant the Ministry of Higher Education (MOHE) for supporting the research work under grant no FRGS/1/2021/STG04/UTM/01/1 and UTM matching grant 04M37.

REFERENCES

[1] N. Kou, S. Yu, Z. Ding, and Z. Zhang, "One-dimensional beam scanning transmitarray lens antenna fed by microstrip linear array," *IEEE Access*, vol. 7, pp. 90731-90740, 2019.

[2] N. Kalva and B. M. Kumar, "Feedline design for a series-fed binomial microstrip antenna array with no sidelobes," *IEEE Antennas Wirel. Propag. Lett.*, vol. 22, no. 3, pp. 650-654, 2023.

[3] B. A. Nia, L. Yousefi, and M. Shahabadi, "Integrated optical-phased array nanoantenna system using a plasmonic Rotman lens," *J. Light. Technol.*, vol. 34, no. 9, pp. 2118-2126, 2016.

[4] Q. Liang, B. Sun, and G. Zhou, "Miniaturization of Rotman lens using array port extension," *IEEE Antennas Wirel. Propag. Lett.*, vol. 22, no. 3, pp. 541-545, 2023.

[5] H. T. Chou and Z. C. Tsai, "Near-field focus radiation of multibeam phased array of antennas realized by using modified Rotman lens beamformer," *IEEE Trans. Antennas Propag.*, vol. 66, no. 12, pp. 6618-6628, 2018.

[6] M. Heino, C. Icheln, J. Haarla, and K. Haneda, "PCB-based design of a beamsteerable array with high-gain antennas and a Rotman lens at 28 GHz," *IEEE Antennas Wirel. Propag. Lett.*, vol. 19, no. 10, pp. 1754-1758, 2020.

[7] J. W. Lian, Y. L. Ban, H. Zhu, and Y. J. Guo, "Reduced-sidelobe multibeam array antenna based on SIW Rotman lens," *IEEE Antennas Wirel. Propag. Lett.*, vol. 19, no. 1, pp. 188-192, 2020.

[8] S. Christie, R. Cahill, N. B. Buchanan, V. F. Fusco, N. Mitchell, Y. V. Munro, and G. Maxwell-Cox, "Rotman lens-based retrodirective array," *IEEE Trans. Antennas Propag.*, vol. 60, no. 3, pp. 1343-1351, 2012.

[9] H. Cho, J. H. Lee, J. W. Yu, and B. K. Ahn, "Series-fed coupled split-ring resonator array antenna with wide fan-beam and low sidelobe level for millimeter-wave automotive radar," *IEEE Trans. Veh. Technol.*, vol. 72, no. 4, pp. 4805-4814, 2023.

[10] S. D. Joseph and E. A. Ball, "Series-fed millimeter-wave antenna array based on microstrip line

structure," *IEEE Open J. Antennas Propag.*, vol. 4, no. pp. 254-261, 2023.

[11] A. Darvazehban, O. Manoochehri, M. A. Salari, P. Dehkhoda, and A. Tavakoli, "Ultra-wideband scanning antenna array with Rotman lens," *IEEE Trans. Microw. Theory Tech.*, vol. 65, no. 9, pp. 3435-3442, 2017.

[12] B. Wang, Z. Zhao, K. Sun, C. Du, X. Yang, and D. Yang, "Wideband series-fed microstrip patch antenna array with flat gain based on magnetic current feeding technology," *IEEE Antennas Wirel. Propag. Lett.*, vol. 22, no. 4, pp. 834-838, 2023.

[13] A. Attaran, R. Rashidzadeh, and A. Kouki, "60 GHz low phase error Rotman lens combined with wideband microstrip antenna array using LTCC technology," *IEEE Trans. Antennas Propag.*, vol. 64, no. 12, pp. 5172-5180, 2016.

[14] S. Ogurtsov and S. Koziel, "A conformal circularly polarized series-fed microstrip antenna array design," *IEEE Trans. Antennas Propag.*, vol. 68, no. 2, pp. 873-881, 2020.

[15] G. Sacco, P. D'Atanasio, and S. Pisa, "A wideband and low-sidelobe series-fed patch array at 5.8 GHz for radar applications," *IEEE Antennas Wirel. Propag. Lett.*, vol. 19, no. 1, pp. 9-13, 2020.

[16] H. T. Chou and C. Y. Chang, "Application of Rotman lens beamformer for relatively flexible multibeam coverage from electrically large-phased arrays of antennas," *IEEE Trans. Antennas Propag.*, vol. 67, no. 5, pp. 3058-3066, 2019.

[17] A. Eid, J. G. D. Hester, and M. M. Tentzeris, "Rotman lens-based wide angular coverage and high-gain semipassive architecture for ultralong range mm-wave RFIDs," *IEEE Antennas Wirel. Propag. Lett.*, vol. 19, no. 11, pp. 1943-1947, 2020.

[18] Karki, S. K., Varonen, M., Kaunisto, M., Rantala, A., Lahti, M., Lamminen, A., & Viikari, V. "Beam-reconfigurable antenna based on vector modulator and Rotman lens on LTCC," *IEEE Access*, vol. 9, pp. 52872-52882, 2021.

[19] J. Y. Deng, Y. Bin Liu, Z. Chen, and W. Lin, "Compact multibeam antenna using miniaturized slow-wave substrate-integrated waveguide Rotman lens for satellite-assisted internet of vehicles," *IEEE Internet Things J.*, vol. 11, no. 4, pp. 6848-6856, 2024.

[20] Y. Liu and M. C. E. Yagoub, "Compact omnidirectional millimeter-wave antenna array fed in series by a novel feed network," *IEEE Trans. Antennas Propag.*, vol. 69, no. 11, pp. 7604-7612, 2021.

[21] Q. Liang, B. Sun, G. Zhou, J. Zhao, and G. Zhang, "Design of compact Rotman lens using truncated ports with energy distribution slots," *IEEE Access*, vol. 7, pp. 120766-120773, 2019.

[22] Y. Kang, E. Noh, and K. Kim, "Design of traveling-wave series-fed microstrip array with a low side-lobe level," *IEEE Antennas Wirel. Propag. Lett.*, vol. 19, no. 8, pp. 1395-1399, 2020.

Abd Al Menam A. Alazzawi earned his B.Eng. degree in Telecommunications from the University of Diyala, IRAQ, in 2015, followed by an M.Eng. degree in Electronics (Telecommunications) from the University of Technology Melaka Malaysia (UTeM) in 2018. Currently, he is pursuing a Ph.D. at the University of Technology Malaysia (UTM) in Johor Bahru city. He is currently conducting research on millimeter waves, base station array antennas, and beamforming circuits.

Mohamad Kamal A. Rahim received the B.Eng. degree in electrical and electronic engineering from the University of Strathclyde, UK, in 1987, the M.Eng. degree in science from the University of New South Wales, Australia, in 1992, and the Ph.D. degree in electrical engineering from the University of Birmingham, UK, in 2003. From 1987 to 1989, he worked as a management trainee with Sime Tyres Mer Gong Alor Star Kedah and as a production supervisor with Sime Shoes, Kulim, Kedah. In 1989, he became an assistant lecturer at the Department of Communication Engineering, Faculty of Electrical Engineering, University Technology Malaysia, Kuala Lumpur. The faculty appointed him as an associate professor. He is currently a professor of RF and antennas at University Technology Malaysia's Faculty of Electrical Engineering.

Osman Ayop earned his B.Eng. degree in electrical engineering, with a major in telecommunication, his M.Eng. degree in RF & Microwave, and his Ph.D. degree in electrical engineering from University Technology Malaysia (UTM) in 2007, 2010, and 2016, respectively. In 2013, he had completed his attachment at Uppsala University, Sweden, under the supervision of Prof. Dr. Vernon Cooray. He is currently a senior lecturer with the Department of Communication Engineering, School of Electrical Engineering, UTM. He is also an active researcher with the Advanced RF and Antenna Research Group (ARFMRG).